



Bound orbits near the throats of phantom scalar field wormholes

I. M. Potashov^a, Ju. V. Tchemarina^b, and A. N. Tsirulev^c

Faculty of Mathematics, Tver State University, Sadovy per. 35, Tver, Russia

e-mail: ^a potashov.im@tversu.ru, ^b chemarina.yv@tversu.ru, ^c tsirulev.an@tversu.ru

Received 30 August 2018, in final form 1 October. Published 4 October 2018.

Abstract. We consider asymptotically flat, static, traversable wormholes supported by a gravitating minimally coupled phantom scalar field with an arbitrary self-interaction potential. It turns out that the main features of bound orbits in wormhole spacetimes are radically different from those in static black hole spacetimes. First, on the throat or near it, there necessarily exists a stable circular orbit in which any test particle has zero angular momentum; this marginal orbit is a degenerate analogue of the innermost stable circular orbit near black holes. Thus, particles of matter resting on these orbits or slowly moving near them can form a thin spherical shell consisting of gas, dust, or fluid. Second, the distance to the throat from an orbit of a test particle with a sufficiently small specific angular momentum can, unlike for the orbits around vacuum black holes, reaches its minimum and maximum values arbitrarily many times (multiple precession — periapsis precession with a very large deficit angle) during one full revolution around the centre.

Keywords: wormhole, phantom scalar field, marginal bound orbits

MSC numbers: 83C10, 83C57

1. Introduction

The compact supermassive objects at the centres of normal galaxies are considered to be surrounded by dense hair of dark matter and today it is still an open question whether they are black holes, naked singularities or wormholes. Observations of bound quasiperiodic timelike orbits play a key role in answering this question and understanding the geometry of spacetime near the centres [1, 2]. On the other hand, in modern astrophysics it is a common point of view that interpretation of the observations should be based on the rigorous mathematical modelling of the central gravitating objects. Within the framework of general relativity and its extensions, there are interesting mathematical models of dark matter in galaxies based on a self-gravitating real scalar field [3, 4, 5]. Any model for a classical (not quantum) traversable wormhole requires violation of the null energy condition [6, 7, 8]. In fact, these models violate all the known local and averaged energy conditions because the null energy condition is the weakest of all classical ones. One of the most natural model of a traversable wormhole is that of a self-gravitating phantom scalar field, which enters the Lagrangian with the negative kinetic term [9, 10, 11, 12, 17]. At present we cannot rule out the possibility that such compact objects exist.

In this article we consider static spherically symmetric phantom scalar field wormholes that connect two opposite asymptotically flat regions. Our main aim is to examine possible types of bound timelike orbits and their special features near the throat for this wide class of traversable phantom scalar field wormholes. So far, this issue has been considered only in a general descriptive mathematical framework by assuming an arbitrary form of the shape function of a static spherically symmetric wormhole [13, 14]. Thus, this inverse modelling presupposes that the spacetime metric has been specified before the solution of field equations, so that the corresponding source (the energy-momentum tensor) of the gravitational field has to be found from the Einstein equations. More interesting and physically motivated problem is considered in Ref. [15], where the authors have studied the geodesic motion in spacetimes describing traversable wormholes supported by a massless conformally-coupled scalar field.

Bound orbits around static and stationary spherically symmetric vacuum black holes are well studied [16]. In contrast, for scalar field wormhole spacetimes, we now have no deeper understanding of the behaviour and the main features even for circular orbits. This is due to the fact that we do not know (in advance, without appealing to observations) the self-interaction potential of a scalar field, regardless of whether we consider it as a really existing field or as a phenomenological model of dark matter. In order to consider the problem in a sufficiently general approach, we use the method developed in Refs. [9, 18, 19, 20, 21, 22] for static spherically symmetric scalar field configurations. We also use the corresponding integral formulas obtained in Refs. [23, 24, 25], which allow us to study bound orbits near the

throats for the arbitrary self-interaction potentials without explicit solving the field equations.

This article is a continuation of our previous publications [26] and [27] in which, respectively, the general problem of circular orbits around static self-gravitating scalar field configurations have been studied and the possibility of oscillations around the marginal circular orbit near a topological geon's surface or a wormhole's throat have been shown. In this article we clear up some details for the issues considered in Ref. [27] and draw particular attention to the bound timelike orbits oscillating around the marginal stable circular orbits, that is, to multiple periapsis precession with a very large deficit angle.

The structure of the article is the following. The next Section contains a preliminary mathematical consideration of static spherically symmetric phantom scalar field wormholes including the choice of a suitable coordinate system, asymptotic conditions, the reduced field equations and the corresponding quadrature formulae. In Section 3 we give a simple classification of qualitatively different types of bound orbits near the throat for wormholes whose opposite asymptotic regions are flat. Section 4 is devoted to studying some analytical illustrative example and to plotting the shape of marginal bound orbits with large angles of periapsis precession.

Throughout the article we adopt the metric signature $(+ - - -)$ and use the geometrical system of units in which $c = 1$ and $G = 1$.

2. Phantom scalar field wormholes

To give a complete picture of a typical static, spherically symmetric wormhole spacetime supported by a phantom scalar field, we should first show that the negative kinetic term in the scalar field Lagrangian is a necessary condition for the existence of such wormholes. We begin with the action

$$\Sigma = \frac{1}{8\pi} \int \left(-\frac{1}{2}S + \varepsilon \langle d\phi, d\phi \rangle - 2V(\phi) \right) \sqrt{|g|} d^4x, \quad (1)$$

where S is the scalar curvature, $\varepsilon = \pm 1$ the sign of the scalar field kinetic term, $V(\phi)$ the self-interaction potential of a scalar field ϕ , and the angle brackets denote the scalar product induced by a given spacetime metric g .

For a static spherically symmetric wormhole spacetime, there exist the most natural coordinates, namely, the so-called quasiglobal coordinates in which the metric has the form

$$ds^2 = A^2 dt^2 - \frac{dr^2}{A^2} - C^2 (d\theta^2 + \sin^2 \theta d\varphi^2), \quad (2)$$

where the metric functions A and C , as well as the field ϕ , are functions of the radial coordinate r with the range from $-\infty$ to ∞ . In the orthonormal basis associated

with the metric (2), the independent field equations for the action (1) are

$$-2A^2 \frac{C''}{C} - (A^2)' \frac{C'}{C} - A^2 \frac{C'^2}{C^2} + \frac{1}{C^2} = \varepsilon A^2 \phi'^2 + 2V, \quad (3)$$

$$(A^2)' \frac{C'}{C} + A^2 \frac{C'^2}{C^2} - \frac{1}{C^2} = \varepsilon A^2 \phi'^2 - 2V, \quad (4)$$

$$-A^2 \phi'' - \phi' \left((A^2)' + 2A^2 \frac{C'}{C} \right) + \varepsilon \frac{dV}{d\phi} = 0, \quad (5)$$

where a prime denotes differentiation with respect to r . Without loss of generality, from now on, we set $r = 0$ on the throats and then $C'(0) = 0$. An evident necessary condition for the existence of traversable wormholes is that $C'' > 0$ in some interval of \mathbb{R}_+ . From equations (3) and (4), we find $C''/C = -\varepsilon \phi'^2$, so that $\varepsilon = -1$ and $C'' \geq 0$ everywhere. It means that scalar field wormholes can be supported only by phantom scalar fields and thus the null energy condition is necessarily violated.

The metric function C increases monotonically with r from the throat to infinity and, taking into account the requirement of asymptotic flatness at infinity, we have the asymptotic behaviour

$$C = r + a + o(1) \text{ as } r \rightarrow \infty, \quad (6)$$

$$C = -r + a^* + o(1) \text{ as } r \rightarrow -\infty. \quad (7)$$

For equations (3) — (5) which are written in the quasiglobal coordinates, we will use the quadrature formulae [25] in the form ($\varepsilon = -1$)

$$\phi' = \sqrt{C''/C}, \quad (8)$$

$$A^2 = 2C^2 \int_r^\infty \frac{r-b}{C^4} dr, \quad (9)$$

$$\tilde{V}(r) = \frac{1}{2C^2} \left(1 - 3C'^2 A^2 - CC'' A^2 + 2C' \frac{r-b}{C} \right), \quad (10)$$

where the parameter b takes arbitrary real values. In order to use the formulas (8) — (10) for obtaining wormhole solutions, it is necessary to specify a monotonically increasing function $C(r)$ satisfying the condition $C'' \geq 0$ on \mathbb{R}_+ and having the asymptotic behaviour (6). Then the field function $\phi(r)$, the metric function A^2 , and the function $\tilde{V}(r)$ can be found from (9) and (10) by direct calculation.

The asymptotic behaviour of the metric function A^2 defines the Schwarzschild mass of the corresponding wormhole spacetime by

$$A^2 = 1 - \frac{2m}{C} + o(1/r), \quad r \rightarrow +\infty. \quad (11)$$

The condition (6) guarantees that m will have the meaning of the Schwarzschild mass. Indeed, substituting the asymptotic expansion (6) into the formula (9) and reexpressing the result as a power series expansion in $1/C$, one obtains

$$A^2 = 1 - \frac{2}{3} \frac{a+b}{C} + o(1/r), \quad r \rightarrow +\infty. \quad (12)$$

Comparing (11) with (12) to first order in $1/C$, we see that

$$m = \frac{a+b}{3}. \quad (13)$$

By exactly the same reasoning, using the asymptotic behaviour (7), one can obtain the analogous result, $m^* = (a^* - b)/3$, for the 'left-hand side' of the wormhole.

3. Types of bound timelike orbits near the throat

In static spacetimes with the metric (2), a massive test particle has the three integrals of motion [26],

$$C^2 \frac{d\varphi}{ds} = J, \quad A^2 \frac{dt}{ds} = E, \quad \left(\frac{dr}{ds} \right)^2 = E^2 - V_{eff}, \quad (14)$$

where J and E are, respectively, the specific angular momentum and the specific energy of the particle, and the effective potential has the form ($k = 1$ and $k = 0$ for timelike and null geodesics, respectively)

$$V_{eff} = A^2 \left(k + \frac{J^2}{C^2} \right). \quad (15)$$

In astrophysical applications of geodesic motion in general relativity, one is mainly interested in studying bound timelike orbits of test particles moving in the central region of a gravitating object. We will restrict our consideration to the central region of a traversable wormhole and to bound orbits near its throat. It will be seen below that near the throat there exist stable circular orbits having zero specific angular momentum $J = 0$ of a test particle (which is at rest) and fully covering a spherical surface of the radius $C(r_{min}) \geq C(0)$ with the corresponding radial coordinate $r_{min} \geq 0$. Below such an orbit is called a marginal circular orbit while bound orbits having zero or small angular momentum and oscillating near a marginal circular orbit are referred to as marginal bound orbits. Note that similar marginal orbits arise in some other spacetimes [28, 29].

The condition $C'(0) = 0$ allows us to continue the function $C(r)$ as an even function in the region $r < 0$. In the other words, we can write this function in the form $C(r) = C_+(r) + \alpha(r)$, where $C_+(r)$ is an even function such that $C(r) = C_+(r)$ for $r \geq 0$, while the bounded function $\alpha(r)$ obeys the conditions

$$\alpha(r)|_{r \geq 0} = 0, \quad \alpha'(0) = 0, \quad \alpha(r) = a^* - a + o(1) \text{ as } r \rightarrow -\infty,$$

so that $\alpha(r) = (\alpha''(0)/2)r^2 + O(r^3)$, $r \rightarrow 0 - 0$. We will restrict our attention to wormholes with positive masses, $m > 0$, and to wormholes with zero mass and the property of gravitational attraction at space infinity. The latter means that $(A^2)' > 0$ in the asymptotic region $r \rightarrow +\infty$. Recall that any wormhole under consideration is traversable and connects, as it has been assumed above, two asymptotically flat regions. Detailed analysis of the quadrature (9) shows, first, that for a given $C(r)$, a solution of the designated kind either does not exist at all or is possible only for a unique value of the parameter b : in the latter case, if $C(r)$ is (or is not) an even function, then $b = 0$ (or, respectively, $b \neq 0$). Second, if $b \neq 0$, the number and mutual location of extrema of A^2 are the same as if there were $C(r) = C_+(r)$ everywhere and, therefore, the qualitative behaviour of the marginal bound orbits is the same. *From now on we suppose $b = 0$ and $a \geq 0$, so that $m = a/3 \geq 0$.*

It is natural to distinguish *two types, say, the first and the second, of marginal circular orbits and associated marginal bound orbits*. We will say that a marginal circular orbit is of the first (respectively, second) type if it as a whole lies in the region $r > 0$ (respectively, if it as a whole lies on the throat). Associated marginal bound orbits of both types lie in some neighbourhood of the marginal circular orbit and cross it an even number of times during either one cycle of radial motion if $J = 0$, or one revolution around the centre if $J > 0$.

Therefore, the function $C(r)$ can be regarded as being exactly or approximately even, depending on whether we are considering a marginal orbit of the first or the second type. It follows directly from (9) that if $b = 0$ and $C(r)$ is even, then A^2 will also be even. From now on we will assume that wormholes possess the reflection symmetry about their throats. Also we exclude from our consideration the special case $A \equiv 1$ (as in the Ellis solution [10]) which admits no bound orbits at all.

From the asymptotic behaviour (11), it is obvious that in some region near the (positive) spatial infinity $(A^2)' > 0$ and therefore A^2 reaches its minimum value at some point $r_{min} \geq 0$ in a coordinate neighbourhood of the throat. Then there exists an integer $n \geq 2$ such that

$$\left\{ (A^2)^{(k)} \right\}_{r=r_{min}} = 0 \quad (k = 1, \dots, n-1), \quad \left\{ (A^2)^{(n)} \right\}_{r=r_{min}} > 0. \quad (16)$$

For the sufficiently general case $n = 2$, these conditions can be written in the explicit form as

$$\left\{ 2 \frac{C'}{C} A^2 - 2 \frac{r}{C^2} \right\}_{r=r_{min}} = 0, \quad (17)$$

$$\begin{aligned} & \left\{ 2 \frac{C''}{C} A^2 - 2 \frac{C'^2}{C^2} A^2 - \frac{2}{C^2} + 4 \frac{C'}{C} \frac{r}{C^2} \right\}_{r=r_{min}} = \\ & = \left\{ 2 \frac{C''}{C} A^2 + 2 \frac{C'^2}{C^2} A^2 - \frac{2}{C^2} \right\}_{r=r_{min}} = \left\{ \frac{1}{C^2} \left((C^2)'' A^2 - 2 \right) \right\}_{r=r_{min}} > 0. \end{aligned} \quad (18)$$

For any wormhole under consideration the first condition in (16) necessarily holds (for some even $n \geq 2$) on the throat ($r = 0$) where the function A^2 has a maximum or a minimum. If the second condition in (16) also holds, then A^2 has a minimum and the corresponding marginal circular orbit lies on the throat and is of second type; otherwise (recalling that we exclude the case $A^2 = 1$) it lies at some radius $C(r_{min})$, $r_{min} > 0$, and is of the first type. In the latter case, r_{min} can be determined by solving equation (17). Thus, in order to determine what type of marginal orbits appears in a wormhole spacetime, we should verify whether the second condition in (16) holds on the throat or not. For $n = 2$ (see the inequality (18)) and $n = 4$, it can be written, more conveniently, in the inverse form

$$\{CC''A^2\}_{r=0} < 1 \quad (n = 2), \quad \{C^2C^{(4)}A^2 - 2C(C'')^2 + 2C''\}_{r=0} < 0 \quad (n = 4); \quad (19)$$

if one of the conditions holds then the corresponding marginal circular orbit lies outside the throat and is of the first type.

4. Analytical examples

In this section we consider some illustrative examples of wormholes having marginal orbits of both the first and the second type and plot the shapes of orbits near the marginal circular ones. The equation for the orbit shapes can be obtained directly from the first integrals of motion (14) in the form

$$\frac{dr}{d\varphi} = \frac{C^2}{J} \sqrt{E^2 - V_{eff}}. \quad (20)$$

On the other hand, in most astronomical applications we are interested in the metric shape function $C(\varphi)$ rather than the coordinate one $r(\varphi)$. Taking this fact into account, for any solution $r(\varphi)$ of equation (20) we will plot the corresponding function $C(r(\varphi))$ on a polar coordinate grid and the corresponding effective potential $V_{eff}(r, J)$ for different values of the specific angular momentum; note that $V_{eff}(r, 0) = A^2(r)$.

4.1 A marginal orbit of the first type (n=2)

In order to explore basic general properties of the shapes of marginal bound orbits, we choose a simple piecewise analytic function $C(r)$ in the form

$$C = \begin{cases} -r - \frac{45}{32}r^{-1} + \frac{9}{4}r^{-3} - \frac{5}{2}r^{-5}, & r < 2; \\ r^4 + \frac{39}{128}r^2 + \frac{93}{64}, & -2 \leq r \leq 2; \\ r + \frac{45}{32}r^{-1} - \frac{9}{4}r^{-3} + \frac{5}{2}r^{-5}, & r > 2; \end{cases} \quad (21)$$

this function as a whole is of class \mathcal{C}^2 . By direct calculation, one can easily verify the fulfilment of the first condition in (19) and find the explicit expressions for the field ϕ (8), the metric function A^2 (8), and the self-interaction potential (10), but they are too unwieldy to be presented here. Instead some features of the marginal bound orbits, mostly informative for the astronomical observations, are plotted in Fig. 1. In particular, the number of periapsis points (nearest to the throat) and the radial distance $C(r_p)$ from the throat to a periapsis point r_p on the marginal bound orbit are increasing when the specific energy E decreases, while the amplitude of oscillations, that is, the radial distance between two neighbouring periapsis and apoapsis points, is decreasing. In a series of numerical experiments, we also have found that the central maximum of the effective potential, $E_J^2 = V_{eff}(r, J)|_{r=0}$, appears to grow monotonically with increasing the specific angular momentum (for not too large values J and such that $E_J^2 > 1$), while the corresponding impact parameter [16], $D^2 = J^2 E_J^2 / (E_J^2 - 1)$, decreases.

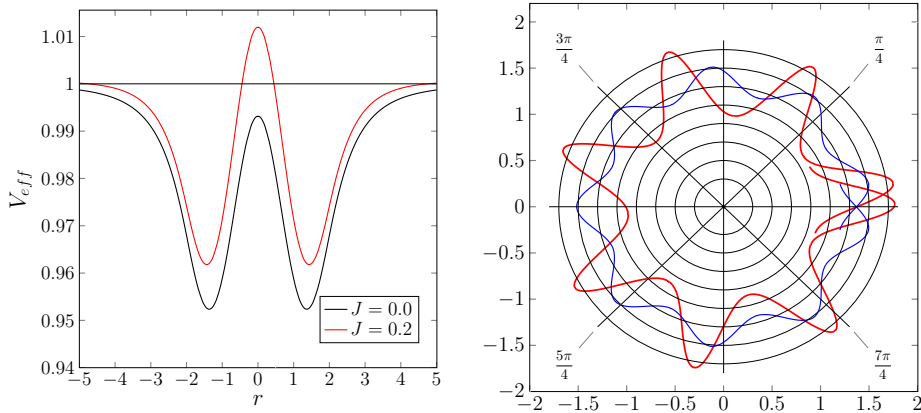


Figure 1: The example (21). Left-hand panel: the effective potentials against radial coordinate r for a test particle with zero specific angular momentum $J = 0$ (black curve, $V_{eff} = A^2$) on the *marginal circular orbit* and for a test particle with $J = 0.2$ (red curve) on the corresponding *marginal bound orbit*. Right-hand panel: the orbital shape $C(\varphi)$ for the two test particles with $E^2 = 0.96$ (red curve) and $E^2 = 0.954$ (blue curve) both having the same specific angular momentum $J = 0.05$.

4.2 A marginal orbit of the first type ($n=4$)

In this subsection we consider the family of the radial functions

$$C = (r^6 + r^4 + b^4 r^2 + a^6)^{1/6}. \quad (22)$$

It is obvious that the case $n = 4$ in (19) can be obtained only by fine tuning of the parameters a and b . By numerical simulations of the corresponding geometry

we have achieved the fulfilment of the condition $CC''A^2|_{r=0} = 1$ and the second condition in (19) with $a = 0.5$, $b = 0.647$. The effective potentials and the orbital shapes are presented in Fig. 2. From this figure, it can be seen that there are no any significant qualitative differences between the cases $n = 2$ and $n = 4$ in the vicinity of the sphere of radius r_{min} . Note that the presence of a maximum of the effective potential with $J > 0$ at some point $r_{max} > r_{min}$ means that in the region $r > r_{max}$ the wormhole will manifest the gravitational repulsion and will have no bound orbits.

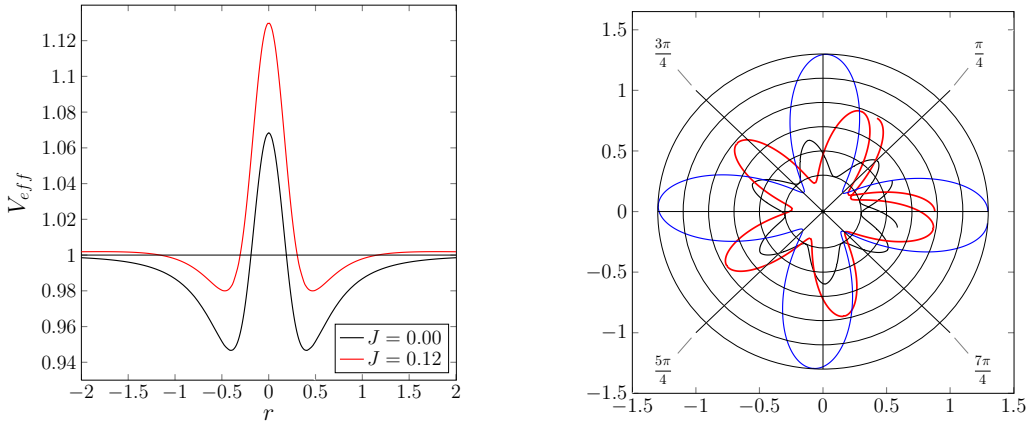


Figure 2: The example (22). On the left-hand side: the effective potentials against radial coordinate r for a test particle with zero specific angular momentum $J = 0$ (black curve) on the *marginal circular orbit* and for a test particle with $J = 0.12$ (red curve) on the corresponding *marginal bound orbit*. On the right-hand side: the orbital shape $C(\varphi)$ for the three test particles with $E^2 = 0.965$ (black line), $E^2 = 0.984$ (red line), and $E^2 = 0.995$ (blue line) all having the same specific angular momentum $J = 0.05$.

4.3 A marginal orbit of the second type ($n=2$)

The family of the radial functions

$$C = ((r^2 + 1)^2 - a^2)^{1/4} + b, \quad 0 \leq a < 1, \quad b \geq 0 \quad (23)$$

gives simple examples of wormholes having marginal circular orbits of the second type. We restrict our attention to massless configurations which are defined by the condition $b = 0$, because they can be treated analytically and their marginal bound orbits have the same qualitative features as those for wormholes with nonzero Schwarzschild mass (13). From (8), (9), and (15) (for timelike geodesic), we find

$$\phi' = -\frac{1}{C^2} \sqrt{1 - 3a^2r^2/C^4},$$

$$A^2 = \frac{C^2}{2a} \ln \frac{r^2 + 1 + a}{r^2 + 1 - a}, \quad V_{eff} = \frac{C^2 + J^2}{2a} \ln \frac{r^2 + 1 + a}{r^2 + 1 - a}.$$

The effective potentials and the orbital shapes are presented in Fig. 3.

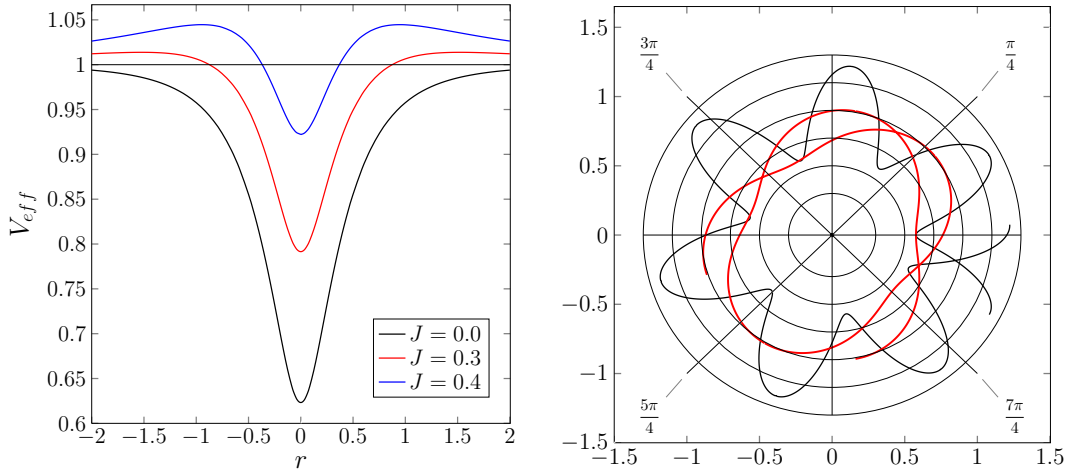


Figure 3: The example (24) with $a^2 = 8/9$, $b = 0$, $E^2 = 0.95$, $J = 0.1$ (black line) and $J = 0.3$ (red line).

5. Conclusions

In this article we have studied circular orbits near the throats of static spherically symmetric wormholes supported by a phantom scalar field minimally coupled to gravity. We have used the quadrature formulas of the scalar field inverse problem method which is applicable to static spherically symmetric configurations. These formulae allow us to consider the orbital problem without preliminary definition of the self-interaction potential of the scalar field. A key feature of the method is its independence from the form of the self-interaction potential.

We have found that bound orbits near the throats of wormholes are radically different from those near event horizons of black holes. On the throat or near it, there necessarily exists a stable circular orbit in which any test particle has zero angular momentum. This marginal orbit is a degenerate analogue of the innermost stable circular orbit near black holes. Particles of matter resting on these orbits can form a thin spherical shell consisting of gas, dust, or fluid. The gas of particles falling little by little into the potential well in a small neighbourhood of such a marginal orbit must have, unlike accretion disks around black holes, an extremely chaotic behaviour. We have also shown that the distance to the throat from an orbit of a test particle with a sufficiently small specific angular momentum can, unlike orbits around vacuum black holes, reaches its minimum and maximum values arbitrarily many times during one full revolution around the centre. In other words, such an orbit has anomalous periapsis precession with a very large deficit angle.

References

- [1] Li Z and Bambi C. *Distinguishing black holes and wormholes with orbiting hot spots*. Phys. Rev. D 2014, **90**, 024071, 11pp ([arXiv: gr-qc/1405.1883](#))
- [2] De Laurentis M, Younsi Z, Porth O, Mizuno Y, Rezzolla L. *Test-particle dynamics in general spherically symmetric black hole spacetimes*. Phys. Rev. D 2018, **97**, 104024, 15pp ([arXiv: gr-qc/1712.00265](#))
- [3] Matos T and Guzmán F S. *On the spacetime of a galaxy*. Class. Quantum Grav. 2001, **18**, pp. 5055 – 5064 ([arXiv: gr-qc/0108027](#))
- [4] Schunck F E and Mielke E W. *General relativistic boson stars*. Class. Quantum Grav. 2003, **20**, pp. 301 – 356 ([arXiv: astro-ph/0801.0307](#))
- [5] Mielke E W, Fuchs B and Schunck F E. *Dark matter halos as Bose-Einstein condensates*, 2006, ([arXiv: astro-ph/0608526](#))
- [6] Morris M S and Thorne K S. *Wormholes in spacetime and their use for interstellar travel: A tool for teaching general relativity*. Am. J. Phys. 1988, **56**, Issue 5, pp. 395 – 412
- [7] Hochberg D and Visser M. *Geometric structure of the generic static traversable wormhole throat*. Phys. Rev. D 1997, **56**, Issue 8, pp. 4745–4755 ([arXiv: gr-qc/9704082](#))
- [8] Visser M. *Lorentzian wormholes: From Einstein to Hawking*. AIP Press, New York, 1995
- [9] Bronnikov K A. *Scalar-tensor theory and scalar charge*. Acta. Phys. Pol. 1973, **B4**, pp. 251 – 266
- [10] Ellis H G. *Ether flow through a drainhole: a particle model in general relativity*. J. Math. Phys., 1973, **14**, pp. 104–118; *Errata*: J. Math. Phys., 1974, **15**, p. 520
- [11] Bronnikov K A and Fabris J C. *Regular fantom black holes*. Phys. Rev. Lett. 2006, **96**, 251101 ([arXiv: gr-qc/0511109](#))
- [12] Bronnikov K A and Sushkov S V. *Trapped ghosts: a new class of wormholes*. Class. Quantum Grav. 2010, **27**, No 9, 095022, 5pp ([arXiv: gr-qc/1001.3511](#))
- [13] Cataldo M, Liempi L, Rodrigues P. *Traversable Schwarzschild-like wormholes*. Eur. Phys. J. C 2017, **77**, Issue 11, 784, 9pp
- [14] Mishra A and Chakraborty S. *On the trajectories of null and timelike geodesics in different wormhole geometries*. Eur. Phys. J. C 2018, **78**, Issue 5, 374, 16pp ([arXiv: gr-qc/11710.06791](#))

- [15] Willenborg F, Saskia Grunau S, Kleihaus B and Kunz J. *Geodesic motion around traversable wormholes supported by a massless conformally-coupled scalar field*. Phys. Rev. D 2018, **97**, issue 12, 124002, 14pp ([arXiv: gr-qc/1801.09769](#))
- [16] Chandrasekhar S. *Mathematical theory of black holes*. Cambridge University Press, Cambridge, UK, 2001
- [17] Bronnikov K A. *Scalar Fields as Sources for Wormholes and Regular Black Holes*. Particles 2018, **1**, Issue 1, pp. 5–32 ([arXiv: gr-qc/1802.00098](#))
- [18] Fisher I Z. *Scalar mesostatic field with regard for gravitational effects*. Zh. Èksper. Teoret. Fiz. 1948, **18**, pp. 636 – 640 ([arXiv: gr-qc/9911008](#))
- [19] Bergmann O and Leipnik R. *Spacetime structure of a static spherically symmetric scalar field*. Phys. Rev. 1957, **107**, pp. 1157 – 1161
- [20] Bechmann O and Lechtenfeld O. *Exact black hole solution with selfinteracting scalar field*. Class. Quantum Grav. 1995, **12**, pp. 1473 – 1482 ([arXiv: gr-qc/9502011](#))
- [21] Dennhardt H and Lechtenfeld O. *Scalar deformations of Schwarzschild holes and their stability* Int. J. Mod. Phys. 1998, **A13**, pp. 741 – 764 ([arXiv: gr-qc/9612062](#))
- [22] Bronnikov K A and Shikin G N. *Spherically symmetric scalar vacuum: no-go theorems, black holes and solitons*. Grav. Cosmol. 2002, **8**, pp. 107 – 116 ([arXiv: gr-qc/0109027](#))
- [23] Tchemarina Ju V and Tsirulev A N. *Spherically symmetric gravitating scalar fields. The inverse problem and exact solutions*. Gravitation and Cosmology 2009, **15**, pp. 94 – 95
- [24] Azreg-Aïnou M. *Selection criteria for two-parameter solutions to scalar-tensor gravity*. Gen. Rel. Grav. 2010, **42**, pp. 1427 – 1456 ([arXiv: gr-qc/0912.1722](#))
- [25] Solovyev D A and Tsirulev A N. *General properties and exact models of static selfgravitating scalar field configurations*. Class. Quantum Grav. 2012, **29**, 055013, 17pp
- [26] Nikonov V V, Potashov I M and Tsirulev A N. *Circular orbits around static self-gravitating scalar field configurations*. Math. Model. Geom. 2016, **4**, No 2 ([mmg.tversu.ru](#))
- [27] Kratovitch P V, Potashov I M, Tchemarina Ju V and Tsirulev A N. *Topological geons with self-gravitating phantom scalar field*. Journal of Physics: Conference Series 2017, **934**, Issue 1, 012047 ([arXiv: gr-qc/1805.04447](#))

- [28] Pugliese D, Quevedo H, and Ruffini R. *Circular motion of neutral test particles in Reissner-Nordström spacetime*. Phys. Rev. D 2011, **83**, 024021 ([arXiv: astro-ph/1003.2687](#))
- [29] Vieira R S S, Schee J, Klužniak W, Stuchlík Z, and Abramowicz M. *Circular geodesics of naked singularities in the Kehagias-Sfetsos metric of Hořava's gravity*. Phys. Rev. D 2014, **90**, 024035, 8pp ([arXiv: gr-qc/1311.5820](#))